Catalytic reaction profile for NADH-dependent reduction of aromatic aldehydes by xylose reductase from *Candida tenuis*

Peter MAYR* and Bernd NIDETZKY*†[1]

*Division of Biochemical Engineering, Institute of Food Technology, University of Agricultural Sciences Vienna (BOKU), Muthgasse 18, A-1190 Vienna, Austria, and †Institute of Biotechnology, Graz University of Technology, Petersgasse 12/I, A-8010 Graz, Austria

Kinetic substituent effects have been used to examine the catalytic reaction profile of xylose reductase from the yeast *Candida tenuis*, a representative aldo/keto reductase of primary carbohydrate metabolism. Michaelis–Menten parameters (k_{cat} and K_m) for NADH-dependent enzymic aldehyde reductions have been determined using a homologous series of benzaldehyde derivatives in which substituents in *meta* and *para* positions were employed to systematically perturb the properties of the reactive carbonyl group. Kinetic isotope effects (KIEs) on k_{cat} and k_{cat}/K_m for enzymic reactions with *meta*-substituted benzaldehydes have been obtained by using NADH ^{2}H-labelled in the pro-*R* C4-H position, and equilibrium constants for the conversion of these aldehydes into the corresponding alcohols (K_{eq}) have been measured in the presence of NAD(H) and enzyme. Aldehyde dissociation constants (K_d) and the hydride transfer rate constant (k_7) have been calculated from steady-state rate and KIE data. Quantitative structure–activity relationship analysis was used to factor the observed substituent dependence of k_{cat}/K_m into a major electronic effect and a productive positional effect of the *para* substituent. k_{cat}/K_m (after correction for substituent position) and K_{eq} obeyed log-linear correlations over the substituent parameter, Hammett σ, giving identical slope values (ρ) of $+1.4$ to $+1.7$, whereas the same Hammett plot for $\log K_d$ yielded $\rho = -1.5$. This leads to the conclusion that electron-withdrawing substituents facilitate the reaction and increase binding to about the same extent. KIE values for k_{cat} (1.8) and k_{cat}/K_m (2.7), and likewise k_7, showed no substituent dependence. Therefore, irrespective of the observed changes in reactivity over the substrate series studied no shift in the character of the rate-limiting transition state of hydride transfer occurred. The signs and magnitudes of ρ values suggest this transition state to be product-like in terms of charge development at the reactive carbon. Structure–reactivity correlations reveal active-site homologies among NADPH-specific and dual NADPH/NADH-specific yeast xylose reductases and across two aldo/keto reductase families in spite of the phylogenetic separation of the host organisms producing xylose reductase (family 2B) and aldehyde reductase (family 1A).

Key words: aldo/keto reductase, structure–reactivity correlation, transition state.

INTRODUCTION

Xylose reductase (XR) from the yeast *Candida tenuis* (CtXR) catalyses the conversion of the open-chain aldehyde form of D-xylose into xylitol via NAD(P)H-dependent, pro-4-*R* stereospecific reduction [1,2]. Formation of xylitol represents the first step of the yeast metabolic pathway for D-xylose. Microbial bioconversion of D-xylose has attracted much interest in biotechnology as a promising route towards ethanol and other value-added compounds [3]. CtXR and the other microbial XRs are members of the aldo/keto reductase (AKR) superfamily of proteins and enzymes. They have been classified on the basis of sequence similarity into family AKR 2B ([4]; see also the permanent AKR website at http://www.med.upenn.edu/akr). Like many other AKRs, in addition to its canonical substrate, D-xylose, CtXR is capable of reducing a broad range of aldehydes whose non-reacting parts represent an extremely wide variety of structural scaffolds [5]. Catalysis to carbonyl group reduction by AKR enzymes is thought to involve the co-operation of four amino acids (Tyr/Lys/Asp/His) [6] which are positionally conserved in the vast majority of reductases of the superfamily [4], and thus members of family AKR 2B. Although somewhat controversial, the phenolic hydroxy group of Tyr is the most likely candidate to function as the general acid/base catalyst of the reaction while the other tetrad residues appear to have auxiliary roles in catalysis [6–10]. The available evidence from biochemical studies [1,2,11] and X-ray structure determination (K. Kavanagh, M. Klimacek, B. Nidetzky and D. Wilson, unpublished work) suggests a basic catalytic mechanism of CtXR common to other AKR members for which structure–function relationships have been established on a molecular level [6–10].

During the NAD(P)H-dependent enzymic reduction of an aldehyde the relative timing of hydride-transfer and proton-transfer steps may be extremely synchronous or fully stepwise, as illustrated in Scheme 1. In AKR catalysis, reduction of the carbonyl substrate is thought to take place by a partially stepwise mechanism in which the hydride transfer proceeds ahead of the proton transfer [6,12–15] (Scheme 1). Both hydrogen-transfer steps may be partially rate-limiting for ternary complex conversion [12–15]. If the reaction was fully stepwise and proton transfer was slow, an enzyme–Tyr–OH · NAD(P)$^+$ · oxyanion complex could have a significant lifetime and thus represent a real catalytic intermediate. If, on the other hand, a large degree of

Abbreviations used: BA, benzaldehyde; 3-X-BA and 4-Y-BA; derivatives of BA substituted at positions 3 or 4 on the aromatic ring; BzOH, benzylalcohol; KIE, kinetic isotope effect; LFER, linear free energy relationship; NADD, 4-*R*-[^{2}H]NADH; QSAR, quantitative structure–activity relationship; XR, xylose reductase; CtXR, *Candida tenuis* XR; CrfXR, *Cryptococcus flavus* XR; CiXR1, NADPH-dependent *Candida intermedia* XR; CiXR2, dual-specificity NADPH/NADH-dependent *Candida intermedia* XR; AKR, aldo/keto reductase.

[1] To whom correspondence should be addressed, at the Institute of Biotechnology, Graz University of Technology (e-mail bernd.nidetzky@tugraz.at).

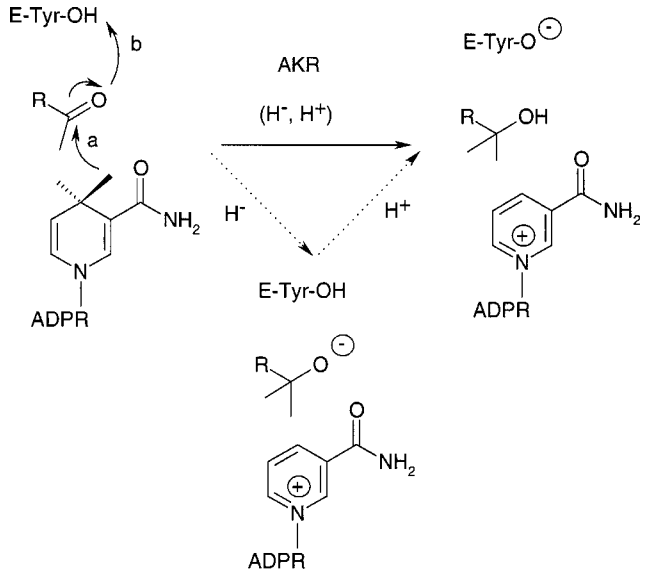

Scheme 1 Mechanism of nicotinamide nucleotide-dependent carbonyl group reduction catalysed by AKRs using general acid catalysis from an enzyme tyrosine

The relative timing of hydride (a) and proton transfer (b) is not known exactly. If the reaction occurred in a fully stepwise fashion by hydride transfer preceding the proton transfer (dotted arrows), an oxyanion intermediate could be formed.

concertedness was present in the chemical steps, the transition state of the reaction could bear partial resemblance, structurally or charge-wise [12], to an enzyme–Tyr–OH · NAD(P)$^+$ · oxyanion complex (Scheme 1). It is, to the best of our knowledge, not known how the chemical steps of AKR catalysis are coupled with charge development at the carbonyl group undergoing reduction, relative to the original carbonyl group in solution or bound to the enzyme active site. In addition, the enzymic mechanism by which some AKR members, including CtXR [15], achieve a very large preference for catalysing the reductive direction of aldehyde/alcohol interconversion is still unresolved [6]. Therefore, a number of mechanistic details of the AKR-catalysed reduction of carbonyl-containing substrates remain to be addressed experimentally.

One approach that may provide direct information on structures of the central complexes and the transition state of an enzymic reaction is adapted from physical organic chemistry. It employs the systematic variation of the structure of the substrate coupled with a thorough search for interpretable quantitative structure–reactivity correlations of kinetic substituent effects. Success of the substrate-modification method depends on the ability of the enzyme to accept a range of substrates representing a wide variety of substituents. It usually requires that steric and bonding factors be small so that the electronic substituent effects controlling the chemical reaction will be clearly expressed in the enzymic rate enhancement. Considering the unusual, but perhaps physiologically relevant [16], tolerance of many AKRs towards variations in the non-reacting portion of the aldehyde substrate, it is surprising that studies of substituent effects on the free energy profile of the reaction, coupled with structure–reactivity analysis of the kinetic consequences, have not been explored systematically to provide answers to the outstanding, significant questions of AKR catalysis and likewise inhibition.

The present paper reports steady-state kinetic parameters for the NAD(P)H-dependent reduction of a homologous series of monosubstituted benzaldehydes (BAs; 3-X-BA and 4-Y-BA, where X or Y = CH_3, OCH_3, H, F, Cl, Br, CN or NO_2) catalysed by CtXR and correlates structural features of the substituent with turnover number, catalytic efficiency and primary deuterium kinetic isotope effects (KIEs) on k_{cat} and $k_{cat}/K_{aldehyde}$. Substrate-binding constants and the hydride-transfer rate constant were calculated from the experimental data, and their substituent dependences were analysed. A quantitative structure–activity relationship (QSAR) approach provided the basic framework for the analysis of the results and was employed to separate electronic substituent effects on kinetic parameters from contributions that are due to bonding [17]. The interpretation of the electronic linear free energy relationships (LFERs) has allowed some new insights into the AKR-catalysed process of carbonyl group reduction. LFERs were also used to measure active-site similarities among four yeast XRs in AKR family 2B and, by using data from the literature [18], among members of AKR families 2B and 1A.

EXPERIMENTAL

Materials and enzymes

BA, 3-X-BA, 4-Y-BA and all other materials were of the highest purity available from Sigma, Fluka or Aldrich. A-side deuterium-labelled NADH (4-*R*-[^{2}H]NADH; NADD) was prepared by reported methods [19]. The incorporation of deuterium in the pro-4-*R* position of NADH was verified by ^{1}H-NMR, and the isotopic purity of NADD was estimated to be greater than 98 %. Deuteriumoxid containing 99.8 % deuterium was obtained from Chemotrade GesmbH (Leipzig, Germany). XRs were obtained from natural yeast sources by using purification protocols reported previously: dual-specificity NADPH/NADH-dependent XR from *C. tenuis* CBS 4435 (CtXR [20]) and *C. intermedia* (CiXR2 [21]), and NADPH-dependent *Cryptococcus flavus* XR (CrfXR [1]) and *C. intermedia* XR (CiXR1 [21]). The XRs were chosen to represent the multiplicity of these reductases in yeast physiology with respect to both coenzyme specificity and multiple isoforms produced by a single organism [1]. A molar extinction coefficient of 54000 $M^{-1} \cdot cm^{-1}$ was used to determine the molarity of stock solutions of CtXR [2]. The Coomassie dye-binding assay from Bio-Rad was used to measure the concentrations of the other XRs, using known concentrations of homologous CtXR as the standard.

Initial rate studies and determination of kinetic parameters

Measurements of the initial rates of aldehyde reduction were performed with a Beckman DU-650 spectrophotometer at 25 °C using NADH or NADPH and monitoring the decrease in absorbance at 340 nm, due to oxidation of the coenzyme (ϵ = 6220 $M^{-1} \cdot cm^{-1}$). The enzyme concentration in the assay was usually $\approx$ 20 nM. Substrate stock solutions were prepared in ethanol and, if required for dissolution, incubated at 55 °C for 2 h. Upon cooling to 25 °C, the solutions were diluted into 50 mM potassium phosphate buffer, pH 7.0, and used immediately for the kinetic measurements. The final ethanol concentration in all assays was constant at 2 % (v/v) and was shown to be without effect on enzyme activity and the kinetic parameters for reactions with D-xylose and BA. If not mentioned otherwise, initial rates were obtained under conditions in which coenzyme concentration was constant and saturating at 200 μM while the concentration of the aldehyde was varied, typically in the range 0.2 $K_{aldehyde}$ to 5 $K_{aldehyde}$. Measurements in the direction of

alcohol oxidation were carried out in the presence of 3 mM NAD^+, which is saturating in coenzyme. The enzyme concentration was in the range 20–30 μM and the concentration of the alcohol was varied between 1 and 10 mM. No ethanol was present in these experiments and the increase in A_{340} was monitored. Primary deuterium KIEs on apparent kinetic parameters for aldehyde reduction by CtXR were obtained by using NADD, employing otherwise identical reaction conditions to those described above. Deuterium solvent KIEs for reduction of BA and 3-F-BA by CtXR were determined at pH (or p^{2}H) of 7.0 using saturating concentrations of NADH and the aldehyde as the varied substrate. p^{2}H in ^2H_2O was adjusted using correction for the isotope effect on the response of the pH electrode according to p^{2}H meter reading $+0.4$. All measurements were done in triplicate and the observed rates were corrected for the appropriate blank readings obtained in controls lacking either the substrate or the enzyme.

Determination of equilibrium constants

The thermodynamic equilibrium constants (K_{eq}) at 25 °C for NADH-dependent reductions of BA, 3-Br-BA, 3-CH_3-BA, 3-NO_2-BA and D-xylose were determined in 50 mM potassium phosphate buffer, pH 7.0 (not containing ethanol), by measuring the oxidation of the corresponding benzylalcohols (BzOHs) and xylitol in the presence of 1–3 mM NAD^+ and 20 μM CtXR. The reduction of NAD^+ was recorded spectrophotometrically over time until A_{340} had reached a constant value. For each BA/BzOH pair, the calculation of K_{eq} was based on four independent determinations in which the concentrations of the alcohols was varied in the range 1–20 mM. K_{eq} was calculated by using the expression $K_{eq} = [BzOH][NAD^+]/([BA][NADH][H^+])$. The relative S.D. values for the reported K_{eq} values were $\leqslant 25\,\%$. It was our experience that utilization of reaction mixtures containing the enzyme and known concentrations of all four reactants and measurement of ΔA_{340} upon attainment of equilibrium did not improve the estimate for K_{eq} in statistical terms.

The relative proportions of aldehyde hydrate in aqueous solutions of BA or a derivative thereof at 25 °C and pH 7.0 were calculated using observed equilibrium free energy changes (ΔG^0) for the conversion of aldehyde into aldehyde hydrate ([22] and supporting information for that paper). Tabulated ΔG^0 values were converted into equilibrium constants (K'_{eq}) with the expression $\Delta G^0 = -RT\ln K'_{eq}$, where K'_{eq} is given by the ratio [aldehyde hydrate]/[aldehyde]. Eqn (1) was used to obtain a percentage value of hydrated aldehyde.

$$\text{Hydrated aldehyde } (\%) = K'_{eq} \cdot 100/(K'_{eq}+1) \quad (1)$$

General analysis of kinetic data

Steady-state kinetic parameters were obtained from unweighted non-linear least-square fits of eqn (2) to initial-rate data which gave linear double-reciprocal plots. The Sigmaplot 2000 program was used and in eqn (2), v is the initial rate, [E] is the molar concentration of the enzyme subunit (36 kDa), [A] is the substrate concentration, k_{cat} is the turnover number (s^{-1}) and K_A is an apparent Michaelis constant.

$$v = k_{cat}[E][A]/(K_A+[A]) \quad (2)$$

In the case when substrate solubility prohibited saturation of the enzyme in aldehyde or alcohol, the catalytic efficiencies ($k_{cat}/K_{aldehyde}$; $k_{cat}/K_{alcohol}$) were calculated from the part of the Michaelis–Menten curve, where v is linearly dependent on the concentration of the varied substrate. The slope of the observed straight line corresponds to the expression $k_{cat}[E]/K$.

KIEs were calculated by fitting eqn (3) to experimental initial-rate data that were obtained under otherwise exactly identical conditions using NADH or NADD. In eqn (3), $E_{V/K}$ and E_V are the isotope effects minus 1 on k_{cat}/K_A and k_{cat}, respectively. F is the fraction of deuterium in the labelled substrate NADD or the solvent.

$$v = k_{cat}[E][A]/\{K_A(1+F\cdot E_{V/K})+[A](1+F\cdot E_V)\} \quad (3)$$

KIEs are reported using the nomenclature of Northrop [23] whereby $^{2H}k_{cat}$ and $^{2H}(k_{cat}/K)$ are primary deuterium KIEs on k_{cat} and k_{cat}/K, respectively, and $^{2H_2O}k_{cat}$ and $^{2H_2O}(k_{cat}/K)$ are solvent deuterium KIEs on the same kinetic parameters.

Calculation of substrate binding constants and hydride-transfer rate constants using KIEs and steady-state kinetic parameters

Klinman and Matthews [24] have shown that KIE data and eqn (4) can be used to obtain estimates for the dissociation constant ($K_{dA} = k_6/k_5$) of the central enzyme–substrate complex undergoing reaction. Note that the rate-constant numbering builds on the expanded ordered Bi Bi kinetic mechanism of CtXR [15] (Scheme 2), which will be referred to later in the discussion.

$$K_{dA} = K_A[^{2H}(k_{cat}/K_A)-1]/(^{2H}k_{cat}-1) \quad (4)$$

Isotope effects on k_{cat} ($^{2H}k_{cat} = 1.55$) and k_{cat}/K_{xylose} [$^{2H}(k_{cat}/K_{xylose}) = 2.09$] for NADH-dependent reactions of CtXR with D-xylose [15], and a value of 76 mM for K_{xylose} are used to calculate a $K_{d\,xylose}$ of 150 mM. This value is in reasonable agreement with a $K_{d\,xylose}$ value of 275 mM obtained from transient-state kinetic data [15] and thus serves to validate the analysis by using eqn (4).

Furthermore, Cook [25] has shown that the isotope effect on k_{cat} can be used to calculate the rate constant of the isotope-sensitive step (k_7) provided that the intrinsic isotope effect on this step is known. Eqn (5) was used with the assumption that $^{2H}k_7 \approx 6.5$, an estimate of the intrinsic isotope effect for NADPH-dependent reduction of D-xylose by human aldose reductase [12].

$$k_7 = k_{cat}(^{2H}k_7-1)/(^{2H}k_{cat}-1) \quad (5)$$

Since we are interested to determine the substituent dependence of the hydride-transfer rate constant, relative values for k_7 are required for enzymic reactions with a series of homologous aldehyde substrates. Determination of an exact value of $^{2H}k_7$ for NADH-dependent reduction of aromatic aldehyde by CtXR is, therefore, not a requirement for the analysis to be valid. We stress, however, that observed KIEs on transient rate constants and steady-state kinetic parameters for CtXR-catalysed reduction of D-xylose in the presence of NADH agree well with the contention that $^{2H}k_7 \approx 6.5$ [15]. Eqn (5) is used to calculate a reference value of $\approx 170\ s^{-1}$ for k_7 in the reaction of CtXR with D-xylose. Note that k_7 is free of kinetic complexity.

QSAR analysis

A basic postulate of QSAR is that complex substituent effects on enzymic rates and equilibrium constants for chemical reactions can be factored into the effect of the substituent on the electronic, hydrophobic and steric characteristics of the parent compound [17]. In a first approximation, the dependence of the experimentally observed parameter on changes in substituent structure can be factored in a linear relationship, as shown in eqn (6). Values for the following substitutent parameters provided the

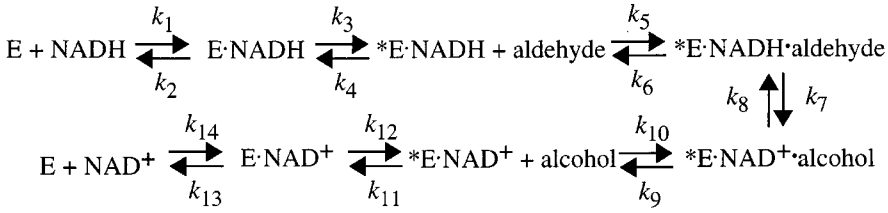

Scheme 2 Kinetic mechanism of NADH-dependent aldehyde reduction catalysed by CtXR, based on data obtained for reactions with D-xylose and xylitol [15]

basic framework for QSAR analysis and were obtained from the literature [17]: Hammett σ and σ^+ for electronic effects; Hansch π for the hydrophobic interaction; Van der Waals radius (V_W), substituent volume (MG_{Vol}) and other parameters for the steric influence. Enzyme catalytic rates (k_{cat}/K_A; k_{cat}), dissociation constants (K_d) or KIEs were correlated with these substituent parameters using this general equation:

$$\log(k_{cat}/K) \text{ (or } k_{cat}, K_d \text{ or KIE)} = \rho\sigma + A\pi + BV_W \text{ (or others)} + \Delta\text{Para (or Meta)} \quad (6)$$

where ρ, A, B and Δ are parameter coefficients, and the parameter Para (or Meta) is utilized to take into account a general positional effect of the substituent. Multiple linear-regression analysis with Sigmaplot 2000 was used to fit eqn (6) to the data. The selection of the best correlation for each set of data was based on a systematic and stepwise procedure which started from single-parameter correlations and added new substituent parameter dependences as required to improve the correlation. The following statistical parameters, provided in the Sigmaplot program report, were used for the assessment of the regression analysis and the resulting structure–reactivity correlation: the coefficient of determination (r^2), which measures how well the regression model describes the data; the standard error of estimate (s), which measures the actual variability about the regression plane of the underlying population; the t test of single parameters; F test for the regression analysis given by the F value; and the significance (P) for each parameter coefficient.

RESULTS

Kinetic parameters for enzymic reduction of substituted BAs

Initial-rate data for enzymic reductions of BA and a series of 14 BA analogues substituted in position 3 or 4 on the aromatic ring were acquired for each of the four yeast XRs, CtXR, CrfXR, CiXR1 and CiXR2. Experimental studies with dual NADPH/NADH-specific CtXR and CiXR2 were carried out by employing NADH. $k_{cat}/K_{aldehyde}$ values derived from initial rate data recorded at a constant saturating concentration of NADPH or NADH showed little ($\leqslant$ 1.5-fold) dependence on the coenzyme used in the experiments, whereby $(k_{cat}/K_{aldehyde})_{NADPH}$ was generally greater than $(k_{cat}/K_{aldehyde})_{NADH}$. Eqn (2) was used to fit the initial-rate data obtained with varied [aldehyde], and the resulting kinetic parameters are summarized in Tables 1 and 2. For each of the four enzymes examined, $k_{cat}/K_{aldehyde}$ showed a strong dependence on the variation of the substituent on the aromatic ring, both in *meta* and *para* positions. The observed changes in catalytic efficiency across the substrate series studied were in a 160–330-fold range and reflect almost entirely reciprocal changes in $K_{aldehyde}$. By contrast, the turnover number showed little variation in response to changes of the substituent on the aromatic ring, as shown for CtXR in Table 1. Average k_{cat} values ($\pm$30 % S.D.) for reduction of BA and derivatives of BA by other yeast XRs were: 25 s^{-1} (CrfXR), 24 s^{-1} (CiXR1) and 8 s^{-1} (CiXR2). Individual XRs differed in the magnitude of their catalytic efficiencies for NAD(P)H-dependent reductions of aromatic aldehydes (Tables 1 and 2). Values of k_{cat}/K_{BA} changed by as much as 26-fold across the series of XRs, equivalent to a differential transition-state-stabilizing binding energy ($\Delta\Delta G^{\ddagger}$) of 8.1 kJ · mol^{-1} (= $RT\ln 26$). Considering the marked constancy of k_{cat}/K_{xylose} within the same group of enzymes [1], the observed $\Delta\Delta G^{\ddagger}$ for BA reduction was unexpected and suggests differences in the capability of each XR to bond productively with BA via hydrophobic and aromatic interactions.

KIE studies

Primary deuterium KIEs on kinetic parameters for the NADH-dependent reductions of 3-X-BA catalysed by CtXR were obtained by comparing initial rates measured in the presence of a constant saturating concentration of NADH and NADD and using the aldehyde as the variable substrate. Eqn (3) was used to fit the experimental data and the resulting KIEs on k_{cat} and $k_{cat}/K_{3\text{-X-BA}}$ are summarized in Table 1. For each substrate examined, the values for $^{2H}k_{cat}$ and $^{2H}(k_{cat}/K_{3\text{-X-BA}})$ were significantly greater than 1, revealing an important contribution of the isotope-sensitive hydride-transfer step to rate limitation for the sequences of reaction steps expressed in the values of k_{cat} and $k_{cat}/K_{3\text{-X-BA}}$ (discussed below). Except for $^{2H}(k_{cat}/K_{3\text{-CH3-BA}})$, which had quite a high value, the observed KIEs on $k_{cat}/K_{3\text{-X-BA}}$ appeared to be essentially independent of structural variations of the aldehyde which over the same substrate series led to a more than 11-fold change in catalytic efficiency. The values of $^{2H}k_{cat}$ in Table 1 show slightly larger variations than the corresponding $^{2H}(k_{cat}/K_{3\text{-X-BA}})$ values. However, changes in $^{2H}k_{cat}$ appear to be unrelated to the electron-withdrawing or electron-donating capabilities of the *meta* substituent. Observed scatter is likely to be a consequence of the poor solubility of some BA derivatives and reflects the requirement for extrapolation when full saturation in aldehyde has not been achieved during initial-rate measurements. Further, Table 1 shows dissociation constants ($K_{d\ 3\text{-X-BA}}$) for central ternary complexes of 3-X-BA and *E · NADH, and rate constants for hydride transfer to 3-X-BA. The K_d values are clearly sensitive to structural variations of the substrate whereas k_7 is not.

Deuterium solvent KIEs on kinetic parameters for NADH-dependent reduction of BA and 3-F-BA were obtained by measuring initial rates in H_2O and ^2H_2O and fitting eqn (3) to the experimental data. $^{2H_2O}(k_{cat}/K_{aldehyde})$ values for reactions with BA and 3-F-BA were 0.91 $\pm$ 0.05 and 0.92 $\pm$ 0.04, respectively. The corresponding values of $^{2H_2O}k_{cat}$ were 1.05 $\pm$ 0.06 and

Table 1 Kinetic parameters for NADH-dependent reduction of BA and derivatives thereof catalysed by CtXR at pH 7.0 and 25 °C

n.a., not applicable.

Substrate	k_{cat} (s^{-1})	$K_{aldehyde}$ (mM)	$k_{cat}/K_{aldehyde}$ ($M^{-1} \cdot s^{-1}$)	$^{2H}k_{cat}$	$^{2H}(k_{cat}/K_{aldehyde})$	k_7 (s^{-1})*	K_d (mM)†
BA	16.6 ± 1.2	15 ± 2	1097	1.51 ± 0.29	2.82 ± 0.35	179	54
4CH_3	15.8 ± 1.0	8.2 ± 0.9	1932				
4OCH_3	n.a.	n.a.	176‡				
4F	18.7 ± 1.1	9.1 ± 0.9	2050				
4Cl	18.5 ± 0.7	1.8 ± 0.2	10572				
4Br	18.1 ± 0.5	1.5 ± 0.1	12378				
4CN	17.2 ± 1.1	1.7 ± 0.2	10131				
4NO_2	22.4 ± 0.9	0.38 ± 0.05	58955				
3CH_3	11.3 ± 1.2	14.4 ± 2.2	788	2.30 ± 0.14	4.65 ± 0.31	48	40
3OCH_3	n.a.	n.a.	257‡				
3F	19.3 ± 1.3	4.7 ± 0.5	4077	1.87 ± 0.13	2.97 ± 0.26	122	10.6
3Cl	13.9 ± 0.6	3.5 ± 0.3	3957	2.00 ± 0.15	2.49 ± 0.20	76	5.2
3Br	15.6 ± 4.1	5.1 ± 1.7	3066	2.34 ± 0.16	2.74 ± 0.18	64	6.6
3CN	19.6 ± 0.7	1.8 ± 0.1	10641	1.52 ± 0.15	2.68 ± 0.28	207	5.8
3NO_2	15.1 ± 1.1	1.2 ± 0.1	12155	1.82 ± 0.10	3.06 ± 0.15	101	3.0

* Calculated by using the data in the Table and eqn (5).
† Calculated by using the data in the Table and eqn (4).
‡ $k_{cat}/K_{aldehyde}$ values calculated from the linear part of the curve in the plot of initial rate versus [aldehyde].

Table 2 $k_{cat}/K_{aldehyde}$ values ($M^{-1} \cdot s^{-1}$) for NAD(P)H-dependent reduction of BA and derivatives of BA catalysed by yeast XRs at pH 7.0 and 25 °C

S.D. were ⩽ 15%.

	$k_{cat}/K_{aldehyde}$ ($M^{-1} \cdot s^{-1}$)		
Substrate	CrfXR	CiXR1	CiXR2
BA	7722	4998	298*
4CH_3	10477	5461	85*
4OCH_3	1355	588	68*
4F	17032	5747	143*
4Cl	45002	22077	231*
4Br	65941	21570	301*
4CN	73148	22265	827*
4NO_2	220066	102521	2401*
3CH_3	5524	2310	658
3OCH_3	2717*	1544*	1127*
3F	24182	18041	707
3Cl	22044	13495	3329
3Br	25840	10827	8281
3CN	56955	44788	9843
3NO_2	42454	52989	18625

* $k_{cat}/K_{aldehyde}$ values calculated from the linear part of the curve in the plot of initial rate versus [aldehyde].

1.05 ± 0.04. The pH profiles of k_{cat} and $k_{cat}/K_{aldehyde}$ for NADH-dependent aldehyde reduction catalysed by CtXR are horizontal on either side of the pH of measurement, pH(D) 7.0 [15]. Therefore, observable solvent KIEs on kinetic parameters for reductions of BA and 3-F-BA should not reflect differences in the pH(D) dependences of k_{cat} and $k_{cat}/K_{aldehyde}$ in H_2O and ^2H_2O.

Enzymic rates of alcohol oxidation

It was difficult to measure precisely at pH 7.0 the initial rates of CtXR-catalysed oxidations of BzOH and monosubstituted BzOH (3-CH_3, 3-Br, 3-NO_2) because the 'alcohol dehydrogenase' activity of CtXR was very small at this pH. Approximate catalytic efficiencies, calculated from linear relationships of initial rates and alcohol concentrations, were 0.2% of the corresponding k_{cat}/K values for reduction of BA. No substituent effect on $k_{cat}/K_{alcohol}$ was detectable.

Structure–reactivity correlations obtained by multiple linear-regression analysis

Initially, an assessment of the dependence of $\log(k_{cat}/K_{aldehyde})$ on the parameters σ (or σ^+), π and V_w was made in single-parameter correlations using the data in Tables 1 and 2. Results of bivariate regression analysis revealed a strong general electronic substituent effect and large steric effect of the methoxy substituents. Unless indicated, kinetic parameters for reactions with 3-CH_3O-BA and 4-CH_3O-BA were, therefore, excluded from all further analyses. LFERs for enzymic reductions of the 3-X-BA and 4-Y-BA series catalysed by CtXR, CrfXR and CiXR1 appeared as roughly parallel lines on Hammett plots of $\log(k_{cat}/K_{aldehyde})$ against the substituent parameter σ (not shown). Therefore, this implies nearly identical $\rho(k_{cat}/K)$ (= slope) values in the *meta* and *para* series and indicates that for these three XRs, the dependence of $k_{cat}/K_{aldehyde}$ on the electron-withdrawing capability of the substituent is virtually identical in both substrate series. The separation between the correlation lines for the 3-X-BA and 4-Y-BA substrate series, Δ, could be factored adequately with the expression, $\log(k_{cat}/K_{4\text{-X-BA}}) = \log(k_{cat}/K_{3\text{-X-BA}}) + \Delta\text{Para}$ whereby the general parameter Para is 1 and 0 for 4-Y-BA and 3-X-BA, respectively. Since 4-Y-BA was the preferred substrate of CtXR, CrfXR and CiXR1, Δ had a positive value (Table 3). The observed specificities for reactions with 4-Y-BA over reactions with 3-X-BA could be partially correlated with the hydrophobicity parameter of the substituent in *para* position (Table 3), probably reflecting greater bonding capabilities of the active sites at this position. The catalytic rates for CiXR2 were higher in the series of *meta*-substituted analogues, and a three-parameter correlation was required to provide a useful fit of the data (Table 3). A Hammett plot for CtXR-catalysed reductions of *meta*-substituted BA derivatives using NADH or NADD is shown in Figure 1. It reveals *protio* and *deuterio* correlations which appear as parallel lines in the Hammett plot and thus yield the same value for

Table 3 Correlations of $k_{cat}/K_{aldehyde}$ for enzymic reductions of substituted BAs with electronic (σ, σ^+), positional (Para, Meta), hydrophobic (π) and steric (VW; Sterimol L; MG_{Vol}) substituent parameters

Equations were fitted to the expression $\log[(k_{cat}/K_{3X(4Y)BA})/(k_{cat}/K_{BA})]$, which was calculated by using the data in Tables 1 and 2. Para indicates a positional substituent parameter whereby Para is 1 and 0 for substrates of the 4YBA and 3XBA series, respectively.

Enzyme	Eqn	Formula	r^2	s	F	P
CtXR	7a	$= 1.43(\pm0.13)\sigma + 0.46(\pm0.09)$Para	0.880	0.188	81	< 0.0001
	7b	$= 1.36(\pm0.15)\sigma^+ + 0.57(\pm0.10)$Para	0.830	0.223	54	< 0.0001
	7c	$= 1.82(\pm0.14)\sigma + 0.66(\pm0.16)\pi$	0.830	0.223	54	< 0.0001
CrfXR	7d	$= 1.23(\pm0.09)\sigma + 0.41(\pm0.06)$Para	0.928	0.123	141	< 0.0001
	7e	$= 1.18(\pm0.10)\sigma^+ + 0.51(\pm0.06)$Para	0.899	0.146	98	< 0.0001
	7f	$= 1.57(\pm0.13)\sigma + 0.49(\pm0.15)\pi$	0.792	0.210	42	< 0.0001
CiXR1	7g	$= 1.43(\pm0.13)\sigma + 0.46(\pm0.09)$Para	0.880	0.188	81	< 0.0001
	7h	$= 1.48(\pm0.09)\sigma + 0.38(\pm0.10)\pi$	0.914	0.142	118	< 0.0001
	7i	$= 1.54(\pm0.11)\sigma^+ + 0.60(\pm0.12)\pi$	0.889	0.162	88	< 0.0001
CiXR2	7j	$= 1.53(\pm0.22)\sigma + 0.44(\pm0.13)VW_{meta} - 0.31(\pm0.11)VW_{para}$	0.879	0.284	44	< 0.0001
	7k	$= 1.48(\pm0.21)\sigma + 0.33(\pm0.07)L_{meta} - 0.22(\pm0.06)L_{para}$	0.932	0.213	42	< 0.0001
	7l	$= 1.48(\pm0.17)\sigma + 3.31(\pm0.56)MG_{Vol,meta} - 2.27(\pm0.49)MG_{Vol,para}$	0.930	0.218	66	< 0.0001

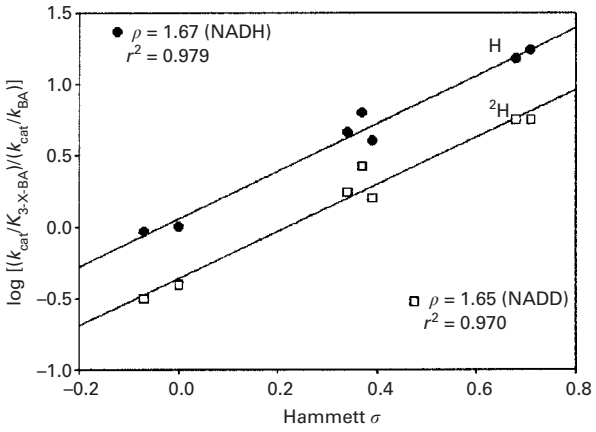

Figure 1 Hammett plot of second-order rate constants for enzymic reductions of 3-X-BA catalysed by CtXR at 25 °C and pH 7.0 using NADH (●) or NADD (□) as the coenzyme

The lines show the best fit of the data in bivariate regression analysis with Hammett σ. Results for reactions with 4-Y-BA were omitted for clarity.

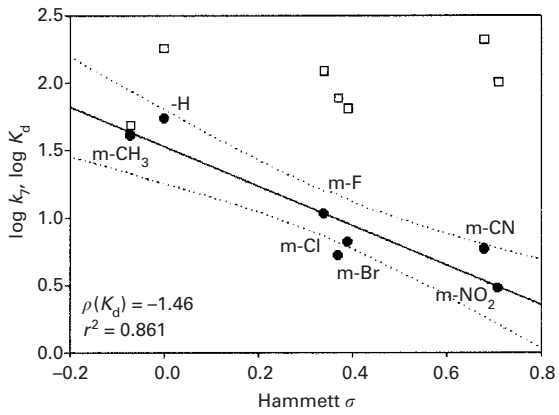

Figure 2 Hammett plot of the dissociation constant for the release of 3-X-BA from the complex with CtXR and NADH (●) and for the hydride-transfer rate constant (□)

The solid line represents the fit of the data for $\log K_{d\ 3\text{-X-BA}}$ in bivariate regression analysis with Hammett σ. The dotted lines show the 95% confidence interval for linear regression. A mean value of 112 s^{-1} provided a statistically adequate description of the data for k_7.

$\rho(k_{cat}/K_{aldehyde})$. Hammett plots for $\log(K_{d\ 3\text{-X-BA}})$ and $\log k_7$ are shown in Figure 2.

Two-parameter correlations for CtXR, CrfXR and CiXR1 were used to obtain final estimates for $\rho(k_{cat}/K_{aldehyde})$ and the results of multiple linear-regression analysis are summarized in Table 3 (eqns 7a–7i). Three- and four-parameter correlations were also examined. However, they typically yielded near-linearly correlated estimates for the parameter coefficients and only slightly better coefficients of determination, clearly indicating that the addition of a third and fourth parameter did not improve the correlation in a statistically significant manner. Structure–reactivity correlations for CiXR2 are shown in eqns (7j)–(7l) (Table 3). They take into account differential steric effects of the *meta* and *para* substituents on the enzymic rate enhancement. Note that in spite of special steric requirements of the CiXR2 active site not observed with the other XR enzymes, there was little variation in the value of the electronic parameter coefficients $\rho(k_{cat}/K_{aldehyde})$ among the four reductases. The r^2 values of between 0.77 and 0.93 together with high F values (> 37) at a very small significance level ($P = 0.0001$) indicate a generally good fit of all equations shown. The results for CtXR, CrfXR and CiXR1 emphasize the actual independence of $\rho(k_{cat}/K_{aldehyde})$ on whether the Hammett σ or σ^+ scale is utilized for structure–activity correlations.

Measurement of active-site similarities among XR enzymes and other AKRs

Two-parameter correlations for CtXR, CrfXR and CiXR1 yielded closely similar parameter coefficients irrespective of the use of the σ/P or σ/π scales (eqns 7a–7i; Table 3). This finding is emphasized by directly correlating the $\log(k_{cat}/K_{aldehyde})$ values, as shown in Figure 3. LFERs of the form $\log(k_{cat}/K_{aldehyde})^{reductase1} = \delta\ \log(k_{cat}/K_{aldehyde})^{reductase2} + \text{constant}$ were used for a general assessment of the active-site similarity between two individual reductases. Slope (δ) values of ≈ 1 (0.88–0.91; $r^2 = 0.95$–0.98) were found for the correlations between CrfXR and CtXR, and CiXR1 and CtXR, and are consistent with the notion that the active sites of these three enzymes are virtually

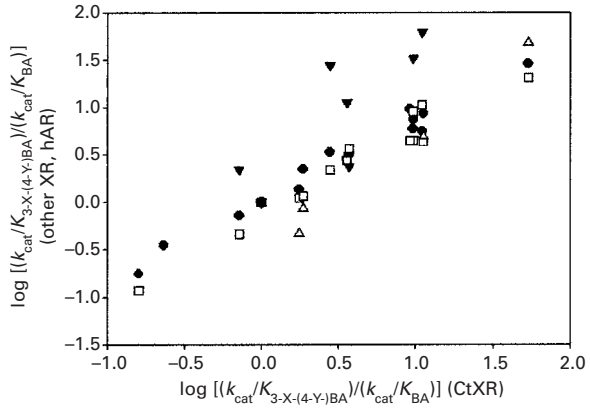

Figure 3 Demonstration of active-site similarities among AKR enzymes by correlating catalytic efficiencies for NAD(P)H-dependent reductions of 3-X-BA and 4-Y-BA

The symbols show $\log(k_{cat}/K_{aldehyde})$ values for CrfXR (●), CiXR1 (□), human aldehyde reductase (hAR; △; data for reductions of 4-Y-BA from [18]) and CiXR2 (▼; data for reductions of 3-CH_3O-BA and 4-CH_3O-BA were not included).

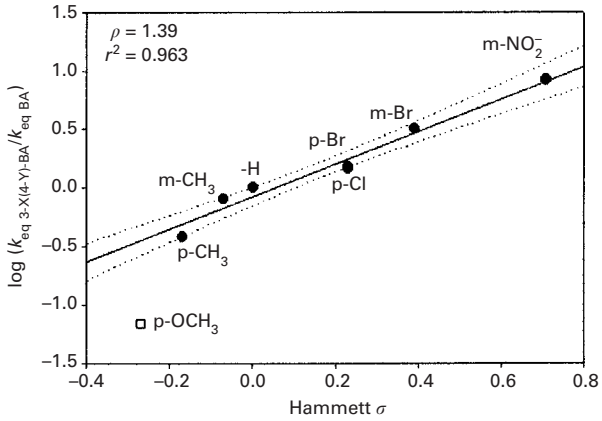

Figure 4 Hammett plot of K_{eq} for the NAD(H)-dependent interconversion of derivatives of BA and BzOH, measured in the presence of CtXR

Values of K_{eq} for *para*-substituted derivatives are from Klinman [26] and the solid line represents the fit of the data in bivariate regression analysis with Hammett σ, omitting results for the *para* methoxy substituent from the analysis. The dotted lines show the 95% confidence interval for linear regression.

Table 4 Equilibrium constants for the conversion of alcohol into aldehyde using NAD^+ in 50 mM potassium phosphate buffer, pH 7.0, and at 25 °C

K_{eq} was calculated by using the relationship $K_{eq} = [\text{alcohol}] \cdot [NAD^+]/[\text{aldehyde}] \cdot [\text{NADH}] \cdot [H^+]$; $K_{eq}[H^+]$ is the equilibrium constant at pH 7.0.

	K_{eq}	$K_{eq}[H^+]$	S.E.M.
BzOH/BA	3.90×10^{10}	3896	286
$3CH_3$BzOH/$3CH_3$BA	3.10×10^{10}	3097	181
3BrBzOH/3BrBA	1.23×10^{11}	12346	3117
$3NO_2$BzOH/$3NO_2$BA	3.24×10^{11}	32448	8214

identical. Data from the literature for human aldehyde reductase (family AKR 1A) [18] were included in Figure 3, and the correlation with CtXR gave a slope value of 1.12 ($r^2 = 0.92$), suggesting that active-site similarity has been conserved across two families of the AKR superfamily. The correlation between CiXR2 and any other XR required correction for steric effects (see Table 3 and Figure 3), and this serves to emphasize peculiarities, probably in the geometry of the substrate-binding site, of CiXR2.

Substituent effects on the equilibrium constant for the NAD(H)-dependent aldehyde/alcohol interconversion

Since equilibrium constants (K_{eq}) for dehydrogenase-catalysed interconversions of carbonyl and alcohol groups are sensitive to changes in the electronic structure of the reactant substituents [26], the dependence of K_{eq} for the reaction, 3-X-BA + NADH + $H^+ \leftrightarrow$ 3-X-BzOH + NAD^+, on the substituent in *meta* position was determined in the presence of CtXR. K_{eq} for the conversion of D-xylose into xylitol was also measured to validate the experimental procedure used for the aromatic reactant systems. Results are shown in Table 4 and indicate clearly that K_{eq} is shifted towards 3-X-BzOH with increasing electron-withdrawing capacity of the substituents. Correlations of $\log K_{eq}$ with Hammett σ yield a $\rho(K_{eq})$ value of 1.40 (results not shown). Klinman [26] reported K_{eq} values for NAD(H)-dependent conversion of 4-Y-BA into 4-Y-BzOH, obtained in the presence of yeast alcohol dehydrogenase. These data fit very well into our correlation of K_{eq} values with Hammett σ (Figure 4). If K_{eq} for the reactant pair, 4-CH_3O-BA and 4-CH_3O-BzOH, is not considered, a $\rho(K_{eq})$ value of 1.39 ($r^2 = 0.963$) is obtained. The direct resonance effect of the *para* methoxy substituent is accounted for in the Hammett σ^+ scale, and correlation of all K_{eq} values measured here and elsewhere [26] with this alternative electronic scale improves the observed r^2 (= 0.996) but yields essentially the same $\rho(K_{eq})$ value of 1.40.

DISCUSSION

In the present paper, we have utilized a LFER approach to characterize the enzymic mechanism of NAD(P)H-dependent aldehyde reduction catalysed by wild-type CtXR, the best described AKR of family AKR 2B. The systematic variation of aromatic-ring substituents ranging from electron-donating to strongly electron-withdrawing has been used as means of perturbing significantly the catalytic reaction profile for reduction of BA by altering the electronic properties of the reactive carbonyl group. Structure–reactivity correlations of substituent effects expressed in steady-state kinetic parameters for aldehyde reductions with *protio* and *deuterio* coenzymes have provided a basic interpretation of reaction co-ordinate interactions and the charge development on the functional carbonyl group undergoing reduction. Another important result of the present study was to demonstrate that LFERs measure sensitively the general active-site similarities among members of family AKR 2B as well as between two different families of the AKR superfamily of proteins and enzymes. The LFERs provide a subtle comparison of two given AKRs based on transition-state structure, information that is not usually obtainable from comparative sequence analysis.

Kinetic and chemical mechanism of CtXR for reaction with D-xylose

The interpretation of LFERs for CtXR-catalysed reduction of aromatic aldehydes builds upon the detailed characterization of the enzymic reaction with the physiological substrate D-xylose

[15]. To provide a comprehensive analysis of structure–reactivity correlations described herein, we review briefly the most relevant findings of the previous paper and emphasize relationships between the reactions with D-xylose and aromatic aldehydes [15]. An expanded ordered Bi Bi kinetic mechanism of CtXR has been proposed based on transient and steady-state kinetic data and is shown in Scheme 2. Steady-state KIE data for enzymic reduction of BA suggest a similar ordered mechanism of CtXR when aromatic aldehydes are the substrates, as follows. The absence of a significant KIE on k_{cat}/K_{NADH} [$^{2H}(k_{cat}/K_{NADH}) = 1.0$] when BA was constant and saturating is in agreement with the requirements of a strictly ordered bi-substrate mechanism where the rate of release of NADH from the ternary enzyme–substrate complex will have a near-zero value. At saturating concentrations of BA, the productive enzyme–NADH complex will display an infinite commitment of undergoing reaction and so the isotope effect on k_{cat}/K_{NADH} is completely masked [25].

In the reaction of CtXR with D-xylose, the conformational step $*E \cdot NAD^+ \rightarrow E \cdot NAD^+$ is mainly, but not fully, rate-limiting for k_{cat}. The partial rate limitation of the turnover number of CtXR by the rate of hydride transfer from NADH is reflected by a value for $^{2H}k_{cat}$ (= 1.6) that is clearly greater than 1. Likewise, a value of 2.1 for $^{2H}(k_{cat}/K_{xylose})$ has revealed a significant contribution of hydride transfer to rate limitation for the catalytic sequence, including all steps from D-xylose binding up to xylitol release. The absence of deuterium solvent isotope effects on k_{cat} and k_{cat}/K_{xylose} has been interpreted to mean that proton transfer which must occur during enzymic reduction of an aldehyde (Scheme 1) is probably not a slow step of the chemical reaction at the active site of CtXR. Different values of $^{2H}(k_{cat}/K_{xylose})$ in H_2O (= 2.1) and ^2H_2O solvent (= 1.6) have suggested a stepwise mechanism of NADH-dependent aldehyde reduction by CtXR in which C–H bond making proceeds ahead of the proton transfer step [15].

Relationship between $k_{cat}/K_{aldehyde}$ and microscopic rate constants

The interpretation of LFERs for steady-state kinetic parameters must consider that k_{cat} and $k_{cat}/K_{aldehyde}$ contain kinetic complexity or, in other words, are functions of several (not just one) microscopic rate constant of which each could display substituent dependence. The kinetic scheme for CtXR (Scheme 2) can be used to derive a quantitative relationship between microscopic rate constants and $k_{cat}/K_{aldehyde}$ (eqn 8).

$$k_{cat}/K_{aldehyde} = k_5/(1+k_4/k_3)[1+(k_6/k_7)(1+k_8/k_9)] \quad (8)$$

In the NADH-dependent reactions of CtXR with D-xylose [15] and most probably other aldehydes, the reverse hydride transfer from alcohol to NAD^+ takes place with a rate constant k_8 that is much smaller than the rate constant k_9 for the dissociation of the alcohol from $*E \cdot NAD^+$ and therefore the value for k_8/k_9 is much smaller than 1 and does not contribute to $k_{cat}/K_{aldehyde}$. In eqn (8), the rate constant ratio k_4/k_3 has a value of ≈ 0.1 and is independent of the aldehyde substrate. Therefore, we may write

$$k_{cat}/K_{aldehyde} \approx 0.9 \cdot k_5/(1+k_6/k_7) \quad (9a)$$

and with $K_{d\ aldehyde} = k_6/k_5$ we obtain

$$k_{cat}/K_{aldehyde} \approx 0.9 \cdot [k_7/(1+k_7/k_6)] \cdot 1/K_{d\ aldehyde} \quad (9b)$$

Hammett plots for $k_{cat}/K_{3\text{-}X\text{-}BA}$ (Figure 1) and $K_{d\ 3\text{-}X\text{-}BA}$ (Figure 2) have revealed identical ρ values, yet with opposite signs. Therefore, structural alterations of the substrate produce reciprocal effects of a closely similar magnitude on catalytic efficiency and the dissociation constant of the central complex. Now, if we consider the absence of a substituent effect on k_7, eqn (9b) implies that the aldehyde 'on' rate (k_5) rather than the 'off' rate (k_6) should be dependent on structural properties of the aromatic ring substituent. Since the free aldehyde appears to be the true substrate of CtXR [1], differences in carbonyl group hydration across a series of homologous aldehydes could affect k_5 (eqn 9a) indirectly. The equilibrium hydration of substituted BA at pH 7.0 and 25 °C was calculated using eqn (1) and is $\approx 1\%$ for BA and 14% for 4-NO_2-BA. Therefore, it almost certainly does not account for the observed substituent effects on $k_{cat}/K_{aldehyde}$.

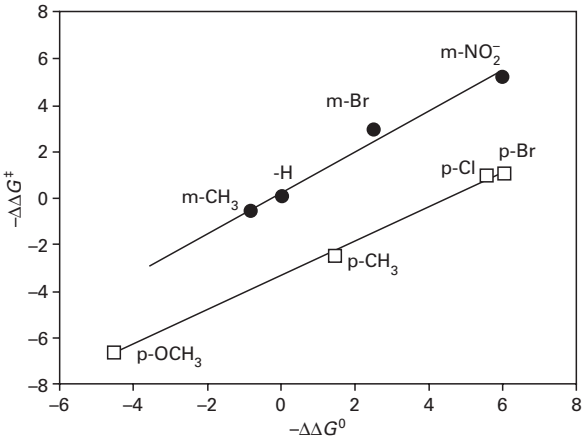

Figure 5 Brønsted plot for NADH-dependent reductions of 3-X-BA and 4-Y-BA catalysed by CtXR at 25 °C and pH 7.0

$\Delta\Delta G^{\ddagger}$ (the incremental Gibbs energy for activation of $k_{cat}/K_{3\text{-}X(4\text{-}Y)\text{-}BA}$) and $\Delta\Delta G^0$ (the incremental Gibbs energy for K_{eq}) were calculated with the expressions $-RT\ln[(k_{cat}/K_{3\text{-}X(4\text{-}Y)\text{-}BA})/(k_{cat}/K_{BA})]$ and $-RT\ln(K_{eq\ 3\text{-}X(4\text{-}Y)\text{-}BA}/K_{eq\ BA})$ using the data in Tables 1 and 4, respectively. The *meta*- and *para*-substituted substrate series (both including BA) are indicated by ● and □, respectively. The lines show the results of linear-regression analysis for the 3-X-BA and 4-Y-BA (excluding BA) substrate series.

Interpretation of electronic LFERs and catalytic reaction profile for CtXR

Hammett plots of the form $\log(k_{cat}/K_{3\text{-}X\text{-}BA})$ versus σ were linear for each of the four yeast reductases studied. The absence of a break in these LFERs is interpreted to indicate that no transitions between different rate-limiting reaction steps occur across the series of homologous substrates. It also implies the underlying chemical mechanism of the enzymes to be unchanged in spite of the altered reactivity of the aldehyde substrates. QSAR analysis for XRs revealed similar values for the electronic parameter coefficient $\rho(k_{cat}/K_{aldehyde})$, suggesting a highly conserved transition state structure.

Substituent effects on $k_{cat}/K_{aldehyde}$ and K_{eq}

The positive values of between 1.4 (Table 3) and 1.7 (Figure 1) for $\rho(k_{cat}/K_{aldehyde})$ show that electron-withdrawing substituents speed the enzymic reductions of 3-X-BA and 4-Y-BA catalysed by CtXR. They suggest an increase in negative charge or, more likely, a decrease in positive charge at the reaction centre upon moving from the free reactants to the transition state. The close similarity of $\rho(K_{eq}) = 1.5$ and $\rho(k_{cat}/K_{aldehyde}) = 1.4$–$1.7$ means that (1) a substitution leading to an incremental change in the binding energy at the transition state produces almost the same effect on the equilibrium constant, and (2) there is a similar charge development at the reactive carbon upon moving along the reaction co-ordinate from $*E \cdot NAD(P)H$ and aldehyde to the

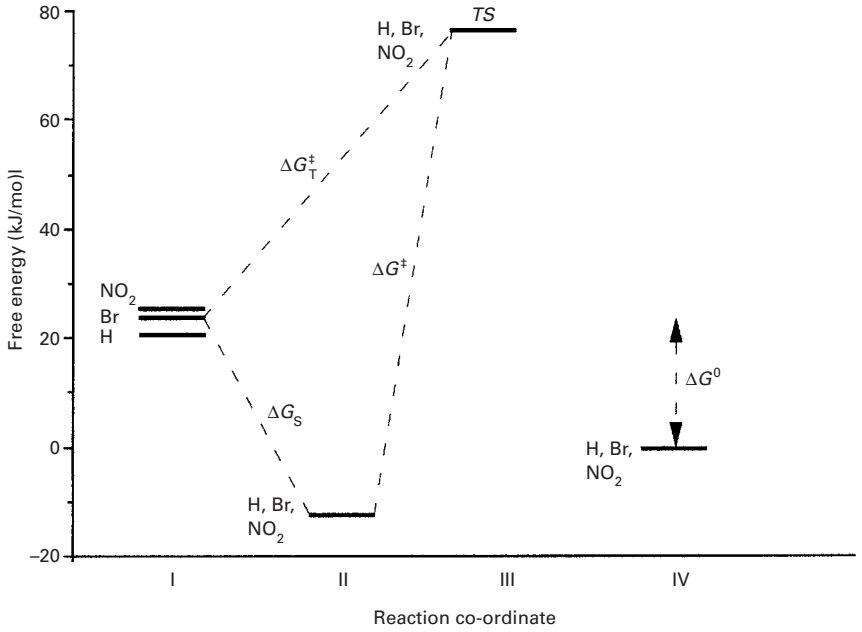

Figure 6 Schematic reaction co-ordinate diagram for the NADH-dependent reduction of 3-X-BA catalysed by CtXR at 25 °C and pH 7.0 based on LFER data and interpretation thereof

In the energy diagram, as one proceeds along the reaction co-ordinate from left to right, one moves from free reactants and enzyme (I) to the central Michaelis complex (II), the transition state (III), and free products and enzyme (IV). A standard free energy of CtXR, NAD^+ and 3-X-BzOH equal to zero and a 1.0 M standard state for substrates and products were assumed. The *meta* substituent is indicated on the left of each energy level. The substituent effect on ΔG^0 ($= -RT\ln K_{eq}$) was assumed to affect the reactant energy level only. The double arrow indicates ΔG^0 for the 3-Br-BA and 3-Br-BzOH system. The Gibbs energies of binding (ΔG_S) and activation for k_{cat}/K ($\Delta G^{\ddagger}_T$) and k_{cat} ($\Delta G^{\ddagger}$) are also indicated by dotted lines. $\Delta G^{\ddagger}_T$ and ΔG_S show substituent dependence whereas $\Delta G^{\ddagger}$ does not.

transition state, and in the reaction equilibrium. A Brønsted plot of the form $-\Delta\Delta G^{\ddagger}$ versus $-\Delta\Delta G^0$ [27] is linear and has a slope (α) whose value is close to 1, as shown in Figure 5 for CtXR-catalysed reductions of the 3-X-BA ($\alpha = 0.88$, $r^2 = 0.99$) and 4-Y-BA ($\alpha = 0.73$, $r^2 = 0.99$) substrate series. This result seems to signify a very product-like transition state in terms of C–H bond formation. The absence of a detectable electronic substituent effect on the catalytic efficiency for the oxidation of 3-X-BzOH is in good agreement with this notion.

Absence of steric substituent effects on $k_{cat}/K_{3\text{-X-BA}}$

The change in hybridization at the reactive centre from planar-sp^2 in aldehyde to pyramidal-sp^3 in primary alcohol could require movements of both active-site groups, the carbon atom undergoing reaction and perhaps the substituted aromatic ring. Klinman [28] has estimated that the displacement of C-4 of the benzene ring of BA could be ≈ 3.5 Å upon conversion into BzOH. Therefore, if geometric and electronic features of a late transition state (in terms of hydride transfer) developed along the reaction co-ordinate in a strongly concerted fashion, one would predict some steric effects on $k_{cat}/K_{aldehyde}$, which were not observed. A product-like transition state structure that is not equally advanced in geometric terms as it is advanced in electronic terms might explain the LEFRs for CtXR. However, we emphasize clearly that multiple measurements of transition-state structure are important to rule out possible ambiguities in the interpretation of structure–reactivity correlations for enzymic reactions (for general discussion, see [26,29]). Also note that the previous discussion is focused on classical views of hydrogen transfer to and from NAD(P)H without the incorporation of quantum-mechanical hydrogen tunnelling [30]. An attractive component of the above transition state is, however, that it predicts the requirement of strain to bring the alcohol into a position poised for reverse reaction at the CtXR active site. A strain mechanism might explain why xylitol shows $\approx$ 3600-fold weaker binding to $*E\cdot NAD^+$ ($K_d = 200$ mM) than the free-carbonyl form of D-xylose binds to $*E\cdot NADH$ ($K_d = 55\ \mu M$) [15].

Substituent effects on KIEs and the hydride-transfer rate constant

The substituent dependencies of $^{2H}(k_{cat}/K_{3\text{-X-BA}})$ and k_7 are both useful to reveal shifts in the character of the transition state that take place in response to an altered intrinsic reactivity of the substrate towards NADH-dependent reduction. For a transition state whose character is unchanged, correlations of $k_{cat}/K_{3\text{-X-BA}}$ for reactions with NADH and NADD with Hammett σ are expected to give essentially parallel lines and thus the same ρ value, as observed in Figure 1. The separation of the two lines measures the KIE on $k_{cat}/K_{3\text{-X-BA}}$ which by itself should not display substituent dependence. The observed constancy of $^{2H}(k_{cat}/K_{3\text{-X-BA}})$ and k_7 across the series of homologous substrates clearly reveals the lack of sensitivity of transition-state character to a substituent effect. We note, however, that the very high value of 4.7 for the KIE on k_{cat}/K for reduction of 3-CH_3-BA does not fit well into the correlation of isotope effects. A reasonable interpretation of this observation cannot be provided at the present time.

Substituent effects on k_{cat} and $K_{d\ 3\text{-X-BA}}$

The absence of a substituent effect on k_{cat} or, in other words, the finding that $\rho(k_{cat}) \approx 0$ would seem to be in conflict with the

observation of a sizable KIE on k_{cat}. However, if we consider that $\rho(K_{d\ 3\text{-X-BA}}) = -1.5$ and $\rho(k_{cat}) = \rho(K_{d\ 3\text{-X-BA}}) + \rho(k_{cat}/K_{3\text{-X-BA}}) = -1.5 + 1.4 \approx 0$, it becomes clear that substituent effects on k_{cat} are cancelled completely by offsetting substituent effects on ground-state binding, as illustrated schematically in Figure 6. The existence of a linear relationship between $K_{d\ 3\text{-X-BA}}$ and Hammett σ suggests that the substituent effect on binding is primarily an electronic one. The sign and magnitude of $\rho(K_{d\ 3\text{-X-BA}})$ reveal that electron-withdrawing groups stabilize the central complex undergoing reaction. This stabilization is apparent because it probably mirrors differences in the energy levels of the free aldehydes in solution (Figure 6). Since aldehyde hydration can be neglected as a direct source of the substituent effect on $K_{d\ 3\text{-X-BA}}$, it would seem that the intrinsic reactivities of 3-X-BA towards CtXR-catalysed reduction are expressed to a very complete extent in the stability of the corresponding ground-state complexes. Once bound to CtXR, these differences in reactivity are eliminated efficiently through positioning at the active site. The negative sign of $\rho(K_{d\ 3\text{-X-BA}})$ is interesting because at face value it is not consistent with the development of electrostatic interactions between the substrate carbonyl and an acidic group on the enzyme upon aldehyde binding to the active site. By way of comparison, binding of aromatic aldehydes to zinc-dependent alcohol dehydrogenase was characterized by a positive value for $\rho(K_{d\ 3\text{-X-BA}})$ or, in other words, favoured by electron-releasing groups on the benzene ring [26]. Polarization of the carbonyl group by an enzyme electrophile to induce charge separation and increase the $^{+}C–O^{-}$ character in the C = O bond is very likely to be an important catalytic factor of CtXR and is expected to occur to some extent at the ground state of reaction. The LFER for $K_{d\ 3\text{-X-BA}}$ may, therefore, be a reflection of other perhaps secondary electronic effects such as destabilizing ground-state strain, for example.

Solvent isotope effects and proton transfer

The values for $\rho(k_{cat}/K_{aldehyde})$ and the solvent isotope effects on the same kinetic parameter for reduction of BA and 3-F-BA provide some, albeit limited, information on the extent of proton transfer in the partially rate-limiting transition state of hydride transfer. The observation of $^{2H_2O}(k_{cat}/K_{BA}) < 1$ rules out a proton in flight as this would be expected to produce a sizable normal isotope effect. It appears not to be consistent with an oxyanion reaction intermediate since a requirement for the intermediate is that proton transfer be a slow step of the chemical reaction. The solvent KIEs may be consistent, however, with a proton nearly fully transferred to the oxygen of the reactive carbonyl group and thus reflect a late transition state of proton transfer. Cancellation of an otherwise sizable deuterium solvent isotope effect on $k_{cat}/K_{aldehyde}$ by a different equilibrium between the free and hydrated forms of the aldehyde in H_2O and ^2H_2O is unlikely. First of all, the values of $^{2H_2O}(k_{cat}/K_{aldehyde})$ for the reduction of BA and 3-F-BA are identical within experimental error although the extent of hydration of the two aldehydes varies to a significant extent ($\approx 10\%$); secondly, a solvent isotope effect on k_{cat}/K_{xylose} was observed only when the hydride transfer was slowed specifically by the use of A-side-labelled NADD [15].

If the same isotope-sensitive step was responsible for the observed solvent isotope effects on k_{cat}/K and k_{cat} in the reactions of CtXR with BA and 3-F-BA, one would expect that $^{2H_2O}(k_{cat}/K_{BA}) \geqslant {}^{2H_2O}k_{cat}$ while it was observed that $^{2H_2O}k_{cat} > {}^{2H_2O}(k_{cat}/K_{BA})$. However, it is important to consider in the analysis of small solvent isotope effects ($\leqslant 1.3$) that the viscosity of ^2H_2O is greater than that of H_2O by about 23% (at 25 °C) [31]. Therefore, the rates of changes in protein structure associated with the coenzyme binding and release steps in ^2H_2O could be altered relative to analogous rates in H_2O. This effect might lead to solvent-dependent conformational equilibria in both E · NADH and E · NAD^+ and is a potential source of the inverse solvent KIE on k_{cat}/K as well as the normal solvent KIE on k_{cat}.

In summary, the results of the present work clearly reveal the dependence of k_{cat}/K for CtXR-catalysed NADH-dependent reduction of aromatic BAs on an electronic substituent effect. They provide an interpretation of how aromatic ring substituents perturb enzyme interactions at different points of the reaction coordinate. It is probably most interesting to note that intrinsic differences in reactivity of the free aldehydes appear to be eliminated completely upon binding to the CtXR active site. Therefore, the rate constant of hydride transfer from NADH does not show a substituent dependence. Any interpretation of LFER data in terms of how far the transition state of hydride transfer is advanced in electronic and geometric terms must be made with great caution. Although the results would seem to be consistent with a late transition state, they clearly do not prove it.

Financial support from the Austrian Science Funds (FWF) grants P12569-MOB and P15208-MOB to B.N. is gratefully acknowledged.

REFERENCES

1 Nidetzky, B., Mayr, P., Hadwiger, P. and Stütz, A. E. (1999) Binding energy and specificity in the catalytic mechanism of yeast aldose reductase. Biochem. J. **344**, 101–108
2 Nidetzky, B., Mayr, P., Neuhauser, W. and Puchberger, M. (2001) Structural and functional properties of aldose (xylose) reductase from the D-xylose-metabolizing yeast *Candida tenuis*. Chem. Biol. Interact. **130–132**, 583–595
3 Aristidou, A. and Penttilä, M. (2000) Metabolic engineering applications to renewable resource utilization. Curr. Opin. Biotechnol. **11**, 187–198
4 Jez, J. M. and Penning, T. M. (2001) The aldo-keto reductase (AKR) superfamily: an update. Chem.-Biol. Interact. **130–132**, 499–525
5 Neuhauser, W., Haltrich, D., Kulbe, K. D. and Nidetzky, B. (1998) Noncovalent enzyme/substrate interactions in the catalytic mechanism of yeast aldose reductase. Biochemistry **37**, 1116–1123
6 Penning, T. M. (1999) Molecular determinants of steroid recognition and catalysis in aldo-keto reductases. Lessons from 3α-hydroxysteroid dehydrogenase. J. Steroid Biochem. Mol. Biol. **69**, 211–235
7 Schlegel, B. P., Jez, J. M. and Penning, T. M. (1998) Mutagenesis of 3α-hydroxysteroid dehydrogenase reveals a 'push-pull' mechanism for proton transfer in aldo-keto reductases. Biochemistry **37**, 3538–3548
8 Lee, Y. S., Hodoscek, M., Brooks, B. R. and Kador, P. F. (1998) Catalytic mechanism of aldose reductase studied by combined potentials of quantum mechanics and molecular mechanics. Biophys. Chem. **70**, 203–216
9 Bohren, K. M., Grimshaw, C. E., Lai, C.-J., Harrison, D. H., Ringe, D., Petsko, G. A. and Gabbay, K. H. (1994) Tyrosine-48 is the proton donor and histidine-110 directs substrate stereochemical selectivity in the reduction reaction of human aldose reductase: enzyme kinetics and crystal structure of the Y48H mutant enzyme. Biochemistry **33**, 2021–2032
10 Tarle, I., Borhani, D. W., Wilson, D. K., Quiocho, F. A. and Petrash, J. M. (1993) Probing the active site of human aldose reductase. J. Biol. Chem. **268**, 25687–25693
11 Klimacek, M., Szekely, M., Griessler, R. and Nidetzky, B. (2001) Exploring the active site of yeast xylose reductase by site-directed mutagenesis of sequence motifs characteristic of two dehydrogenase/reductase family types. FEBS Lett. **500**, 149–152
12 Grimshaw, C. E., Bohren, K. M., Lai, C.-J. and Gabbay, K. H. (1995) Human aldose reductase: rate constants for a mechanism including interconversion of ternary complexes by recombinant wild-type enzyme. Biochemistry **34**, 14374–14384
13 Ma, H., Ratnam, K. and Penning, T. M. (2000) Mutation of nicotinamide pocket residues in rat liver 3 α-hydroxysteroid dehydrogenase reveals different modes of cofactor binding. Biochemistry **39**, 102–109
14 Varnai, P. and Warshel, A. (2000) Computer simulation studies of the catalytic mechanism of human aldose reductase. J. Am. Chem. Soc. **122**, 3849–3860

15 Nidetzky, B., Klimacek, M. and Mayr, P. (2001) Transient-state and steady-state kinetic studies of the mechanism of NADH-dependent aldehyde reduction catalyzed by xylose reductase from the yeast *Candida tenuis*. Biochemistry **40**, 10371–10381
16 Grimshaw, C. E. (1992) Aldose reductase: model for a new paradigm of enzymic perfection in detoxification catalysts. Biochemistry **31**, 10139–10145
17 Hansch, C. and Leo, A. (1995) Exploring QSAR, ACS Professional Reference Book, ACS, Washington DC
18 Bhatnagar, A., Liu, S.-Q. and Srivastava, S. K. (1991) Structure-activity correlations in human kidney aldehyde reductase-catalyzed reduction of para-substituted benzaldehyde by 3-acetyl pyridine adenine dinucleotide phosphate. Biochim. Biophys. Acta **1077**, 180–186
19 Mostad, S. B. and Glasfeld, A. (1993) Using high field NMR to determine dehydrogenase stereospecificity with respect to NADH. J. Chem. Educ. **70**, 504–506
20 Neuhauser, W., Haltrich, D., Kulbe, K. D. and Nidetzky, B. (1997) NAD(P)H-dependent aldose reductase from the xylose-assimilating yeast *Candida tenuis*. Biochem. J. **326**, 683–692
21 Mayr, P., Brüggler, K., Kulbe, K. D. and Nidetzky, B. (2000) Xylose metabolism in *Candida intermedia*: efficient isolation and characterisation of two aldose reductases with different coenzyme specificities. J. Chromatogr. B **737**, 195–202
22 Guthrie, J. P. and Pitchko, V. (2000) Hydration of carbonyl compounds, an analysis in terms of no barrier theory: prediction of rates from equilibrium constants and distortion energies. J. Am. Chem. Soc. **122**, 5520–5528
23 Northrop, D. B. (1982) Deuterium and tritium kinetic isotope effects on initial rates. Methods Enzymol. **87**, 607–625
24 Klinman, J. P. and Matthews, R. G. (1985) Calculation of substrate association constants from steady state isotope effects in enzyme-catalyzed reactions. J. Am. Chem. **107**, 1058–1060
25 Cook, P. F. (1991) Kinetic and regulatory mechanisms of enzymes from isotope effects. In Enzyme Mechanisms From Isotope Effects (Cook, P. F., ed.), pp. 203–230, CRC Press, Boca Raton
26 Klinman, J. P. (1972) The mechanism of enzyme-catalyzed reduced nicotinamide adenine dinucleotide-dependent reactions. J. Biol. Chem. **247**, 7977–7987
27 Kresge, A. J. and Silverman, D. N. (1999) Application of Marcus rate theory to proton transfer in enzyme-catalyzed reactions. Methods Enzymol. **308**, 276–291
28 Klinman, J. P. (1976) Isotope effects and structure-reactivity correlations in the yeast alcohol dehydrogenase reaction. A study of the enzyme-catalyzed oxidation of aromatic alcohols. Biochemistry **15**, 2018–2026
29 Sinnott, M. L., Garner, C. D., First, E. and Davies, G. (1998) Linear free energy relationships. In Comprehensive Biological Catalysis: a Mechanistic Reference, vol. IV (Sinnott, M. L., ed.), pp. 58–65, Academic Press, San Diego
30 Kohen, A. and Klinman, J. P. (1998) Enzyme catalysis beyond classical paradigms. Acc. Chem. Res. **31**, 397–404
31 Quinn, D. M. and Sutton, L. D. (1991) Theoretical basis and mechanistic utility of solvent isotope effects. In Enzyme Mechanism From Isotope Effects (Cook, P. F., ed.), pp. 73–126, CRC Press, Boca Raton

Received 11 January 2002/30 April 2002; accepted 10 May 2002
Published as BJ Immediate Publication 10 May 2002, DOI 10.1042/BJ20020080